Equilibrium of Helicity-driven Spherical Torus Based on Two-fluid Model with Flow

T. Kanki[1], M. Nagata[2], and T. Uyama[2]

[1]*Japan Coast Guard Academy*

[2]*University of Hyogo*

US-Japan exchange 2004
New direction and physics for compact toroids
at LaFonda Hotel, Santa Fe, NM, Sep. 14-16, 2004

Background

Observation of rotating n=1 mode during CHI

--- Toroidal ion flow related to the *n*=1 mode is observed in many ST experiments such as CTX, HIST, SPHEX, SSPX, HIT, and NSTX.

--- This mode is consider to be playing an important role in the current drive mechanism for CHI.

--- On the HIT experiments, the electron fluid at edge regions appears to be locked to the *n*=1 magnetic field structure, suggesting the two-fluid effects.

--- The two-fluid effects are expected to explain the stability of high-β ST.

--- It is necessary to incorporate the two-fluid effects into the helicity-driven equilibrium.

Purpose

--- The details of how such the flowing two-fluid model affects the MHD equilibrium configurations of helicity-driven ST are not investigated numerically.

--- The purpose of this study is to numerically determine the flowing two-fluid equilibrium configurations of the HIST device and to explore their fundamental properties.

--- We focus our attention on the contribution of the ion flow to the configuration, the two-fluid effects, and the β value.

HIST experimental device

Spherical Torus for Coaxial Helicity Injection

R~0.30 m, a~0.24 m, A~1.25, $B_{t.a}$~0.2 T

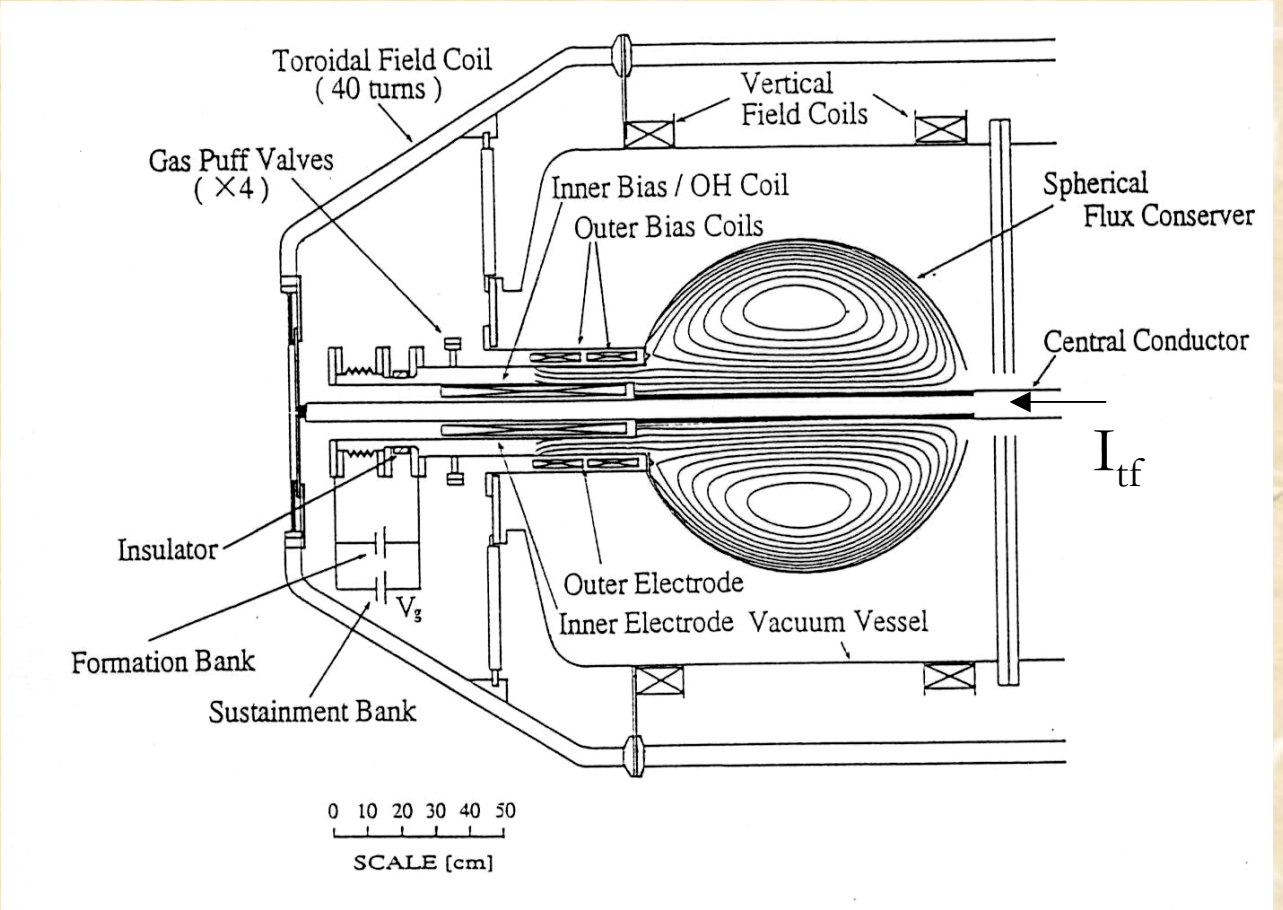

--- The HIST uses the MCPG to produce and sustain the ST plasmas. The plasma formed in the gun is ejected into the FC. After that the ST configuration is generated there and then sustained by CHI.

--- Operation

I_{tf}>0: Tokamak

I_{tf}=0: Spheromak

I_{tf}<0: RFP

Equilibrium equations of flowing Two-fluid

Assumption: $n_i \cong n_e \cong n = \text{Constant}$

NOTE! All quantities of the following equations are normalized.

$\mathbf{u}_\alpha \times \mathbf{\Omega}_\alpha = \nabla H_\alpha \quad (\alpha = i \text{ or } e)$:general equilibrium equations

where $\mathbf{\Omega}_\alpha = \nabla \times \mathbf{P}_\alpha = \nabla \times \mathbf{u}_{\alpha 0} + q_\alpha \mathbf{B}$:generalized vorticity

$H_\alpha \equiv p_\alpha + u_\alpha^2 / 2 + q_\alpha \phi_E$:generalized enthalpy

--- continuity equations of fluid species: $\nabla \cdot \mathbf{u}_\alpha = 0$

--- Gauss' law of magnetism: $\nabla \cdot \mathbf{B} = 0$

--- steady Faraday's law: $\nabla \times \mathbf{E} = 0$

--- Ampere's law: $\nabla \times \mathbf{B} = S_* (\mathbf{u}_i - \mathbf{u}_e)$

H. Yamada *et al*., Phys. Plasmas **9**, 4605 (2002).

Axisymmetric equilibrium equations

Introducing surface functions for the divergence free quantities,

$$\mathbf{B}(r,z) = \nabla\psi(r,z)\times\hat{\boldsymbol{\theta}}/r + B_\theta\hat{\boldsymbol{\theta}} \qquad \mathbf{u}_\alpha(r,z) = \nabla\psi_\alpha(r,z)\times\hat{\boldsymbol{\theta}}/nr + u_{\alpha\theta}\hat{\boldsymbol{\theta}}$$

$$\boldsymbol{\Omega}_\alpha(r,z) = q_\alpha\nabla\Psi_\alpha(r,z)\times\hat{\boldsymbol{\theta}}/r + \Omega_{\alpha\theta}\hat{\boldsymbol{\theta}}$$

Coupled equations for the surface functions of the generalized vorticities, Ψ_i and $\Psi_e(=\psi)$

$$r^2\frac{d\psi_i}{d\Psi_i}\nabla\bullet\left(\frac{d\psi_i}{d\Psi_i}\frac{\nabla\Psi_i}{r^2}\right) = S_*^2(\psi_i-\psi_e)\frac{d\psi_i}{d\Psi_i} + S_*^2(\Psi_e-\Psi_i) + r^2\frac{dH_{i0}}{d\Psi_i}$$

$$\Delta^*\Psi_e = S_*^2(\psi_i-\psi_e)\frac{d\psi_e}{d\Psi_e} + S_*^2(\Psi_e-\Psi_i) - r^2\frac{dH_{e0}}{d\Psi_e}$$

total enthalpies: $H_{\alpha 0}(\Psi_\alpha) = p_{\alpha 0} + \frac{u_{\alpha 0}^2}{2} + q_\alpha\phi_{E0}$

flow stream functions: $\psi_\alpha = \psi_\alpha(\Psi_\alpha)$

Arbitrary functions of Ψ_α

- - - Normalization - - -

We normalize the physical quantities on the basis of the following quantities.

R : radius of the flux conserver

B_R : Poloidal field at the outer boundary on a midplane plane ($r = R$, $z = 0$)

$$V_A = B_R \Big/ \sqrt{\mu_0 m_i n}$$: Alfven velocity

$$S_* \equiv \frac{R}{\ell_i}$$

$$\ell_i = \frac{c}{\omega_{pi}} = \sqrt{\frac{m_i}{\mu_0 n e^2}}$$: ion skin depth

HIST experiment : $n = 5 \times 10^{19}\ \mathrm{m}^{-3} \rightarrow S_* \cong 16$

Differences between single- and two-fluid models

The motion of equation is same for both models.

$$\left[\partial \mathbf{u}_i / \partial t + \mathbf{u}_i \cdot \nabla \mathbf{u}_i\right] = -\nabla(p_i + p_e) + (\nabla \times \mathbf{B}) \times \mathbf{B}$$

$$\mathbf{E} + S_* \mathbf{u}_i \times \mathbf{B} + \mathbf{F}_{2F} = 0$$

two-fluid effect:

gradient of electron pressure and Hall effect

$$\mathbf{F}_{2F} \equiv \nabla p_e - (\nabla \times \mathbf{B}) \times \mathbf{B}$$

$$= -\nabla\left(p_i + \frac{u_i^2}{2}\right) + \frac{\partial \mathbf{u}_i}{\partial t} - \mathbf{u}_i \times (\nabla \times \mathbf{u}_i)$$

The difference between the two- and single- fluid models is the correction term $\mathbf{F}_{2F}$ in Ohm's law which represents the gradient of electron pressure and the Hall effect.

When the following condition holds:

single-fluid assumption : $\boldsymbol{E} \approx S_* \boldsymbol{u}_i \times \boldsymbol{B} >> \boldsymbol{F}_{2F}$

the single-fluid model is adequate.

Numerical model

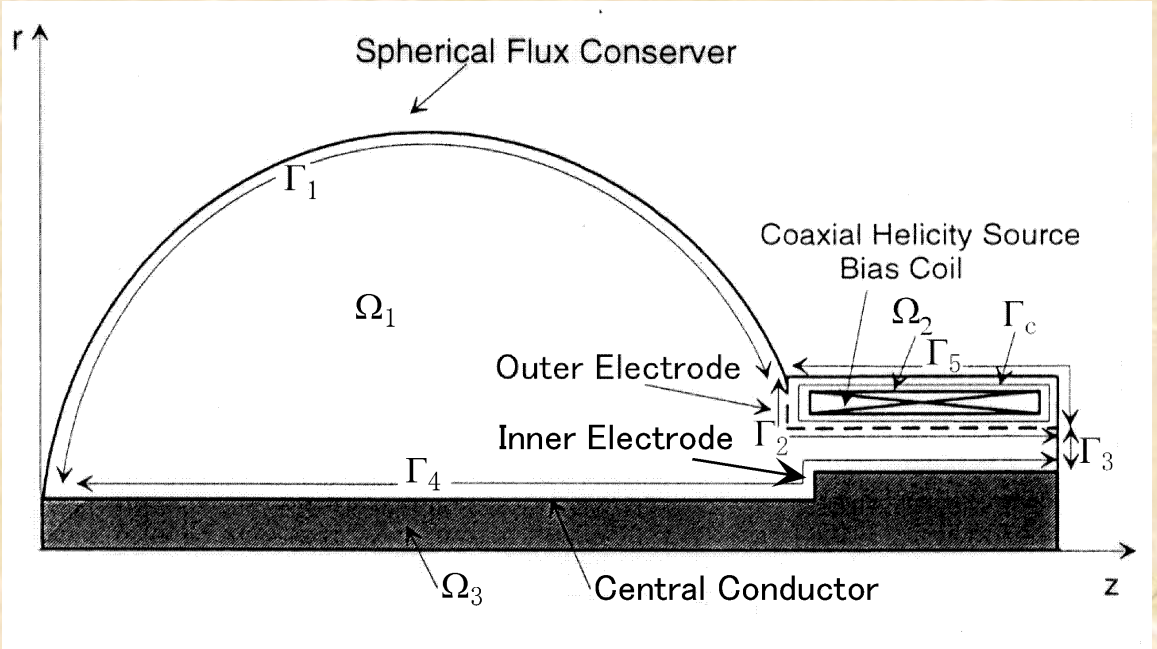

We model the coaxial helicity source and the FC of the HIST by the following assumptions.

Assumption:

--- The bias field penetrates the FC wall, the electrodes, and the central conductor, and further extends all over the space.

--- The magnetic fields generated by the plasma current penetrate the outer electrode.

Assumption and boundary conditions

Assumption:

$$dH_{i0}/d\Psi_i = C_{Hi0} + C_{Hi1}\Psi_i,$$

$$dH_{e0}/d\Psi_e = C_{He0} + C_{He1}\Psi_e + C_{He3}\Psi_e^3,$$

$$\psi_e(\Psi_e) = C_{BT} + C_{\psi e1}\Psi_e + C_{\psi e2}\Psi_e^2$$

Purely toroidal ion flow: $\psi_i(\Psi_i) = 0$

Boundary Condition:

$$\Psi_e = \Psi_{bias} \quad \text{on } \Gamma_1, \Gamma_3, \Gamma_4, \text{ and } \Gamma_5$$

Ampere's law on the coil surface Γ_c can be written as

$$I_{bias} = \oint_{\Gamma_c} \frac{1}{r}\frac{\partial \Psi_e}{\partial n} dl$$

The boundary condition for Ψ_e on the coil surface Γ_c is obtained by setting at unknown constant.

---- For the purpose of computing equilibria, we assume the total enthalpies and the flow stream functions as the surface functions of the vorticities. Here the various C's are constant parameters. Especially, C_{Hi1} is related to the strength of ion flow. We change only this parameter.

--- We consider the special case of purely toroidal ion flow.

Equilibrium computation

--- 2-D ST equilibrium (HIST Devise) can be determined by the combination of FDM and BEM.

--- The constraint condition of this computation is that total toroidal current I_t = const.

For each equilibrium, global quantities are calculated below:

Volume average β value

$$<\beta> \equiv \frac{<p_i + p_e>}{<p_i + p_e + \frac{B^2}{2\mu_0}>}$$

Volume average λ value

$$<\lambda> \equiv \mu_0 \frac{<\mathbf{j}\cdot\mathbf{B}>}{<B^2>}$$

two-fluid index*: $f_{2F} \equiv \frac{<|\mathbf{F}_{2F} \times \mathbf{B}|>}{<|\mathbf{E} \times \mathbf{B}|>}$

If $f_{2F} \geq 1 \, (f_{2F} << 1)$, the two-fluid effect is significant (negligible).

*Remember $\mathbf{E} + S_* \mathbf{u}_i \times \mathbf{B} + \mathbf{F}_{2F} = 0$

Parameters

C_{Hi1}	$S_* C_{BT}$	$<\beta>$	f_{2F}	$<\beta_T>$	β_N	$<\lambda>$
1.0	-0.240	2.30×10^{-2}	1.83	8.11×10^{-2}	1.55	1.32
9.2	-5.02×10^{-3}	0.146	2.82			2.22
15.0	0.215	0.230	1.87			2.24
28.0	0.926	0.179	1.50	0.153	11.3	-0.673

$$C_{Hi0} = 0, \quad C_{He0} = 0, \quad C_{He1} = 4.0, \quad C_{He3} = -1.0, \quad S_* C_{\psi e1} = -0.7, \quad S_* C_{\psi e2} = 0$$

$$I_{bias} / I_t = 2.0$$

We increase the value of C_{Hi1} related to the strength of ion flow to investigate the variation of the magnetic configuration.

Magnetic field profiles on the midplane

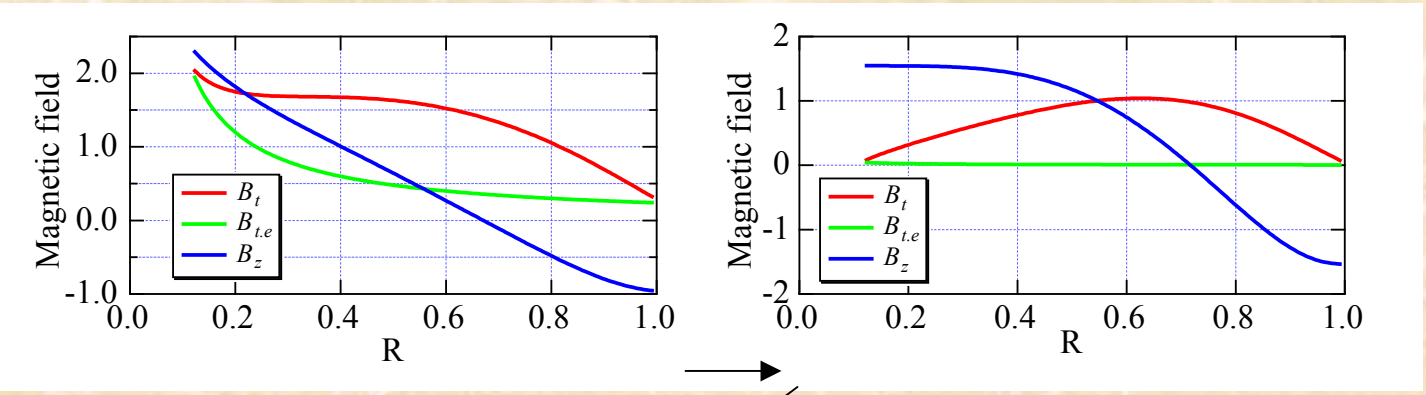

(a) high-*q* ST

(b) Spheromak

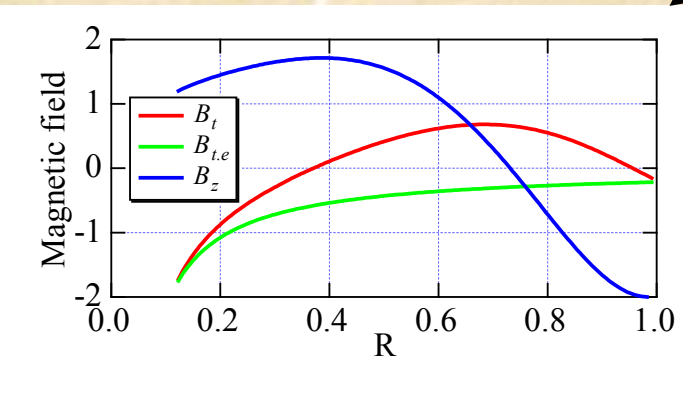

(c) RFP

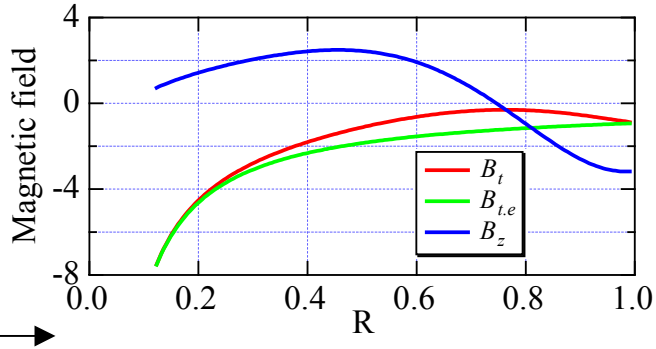

(d) ultra low-*q* ST

--- Figure (a) shows the case of small ion flow and the high-*q* ST with paramagnetic B_t profile.
--- As the effect of ion flow becomes more significant, $B_{t.e}$ decreases and further reverses its sign.
--- Figure (b) shows the spheromak without $B_{t.e}$.
--- In Fig. (c) B_t at the edge regions reverses the sign, which indicates the RFP-like configuration.
--- In Fig. (d) B_t at the whole regions reverses the sign, which indicates the ultra low-*q* ST with diamagnetic B_t profile.

Flow velocity profiles on the midplane

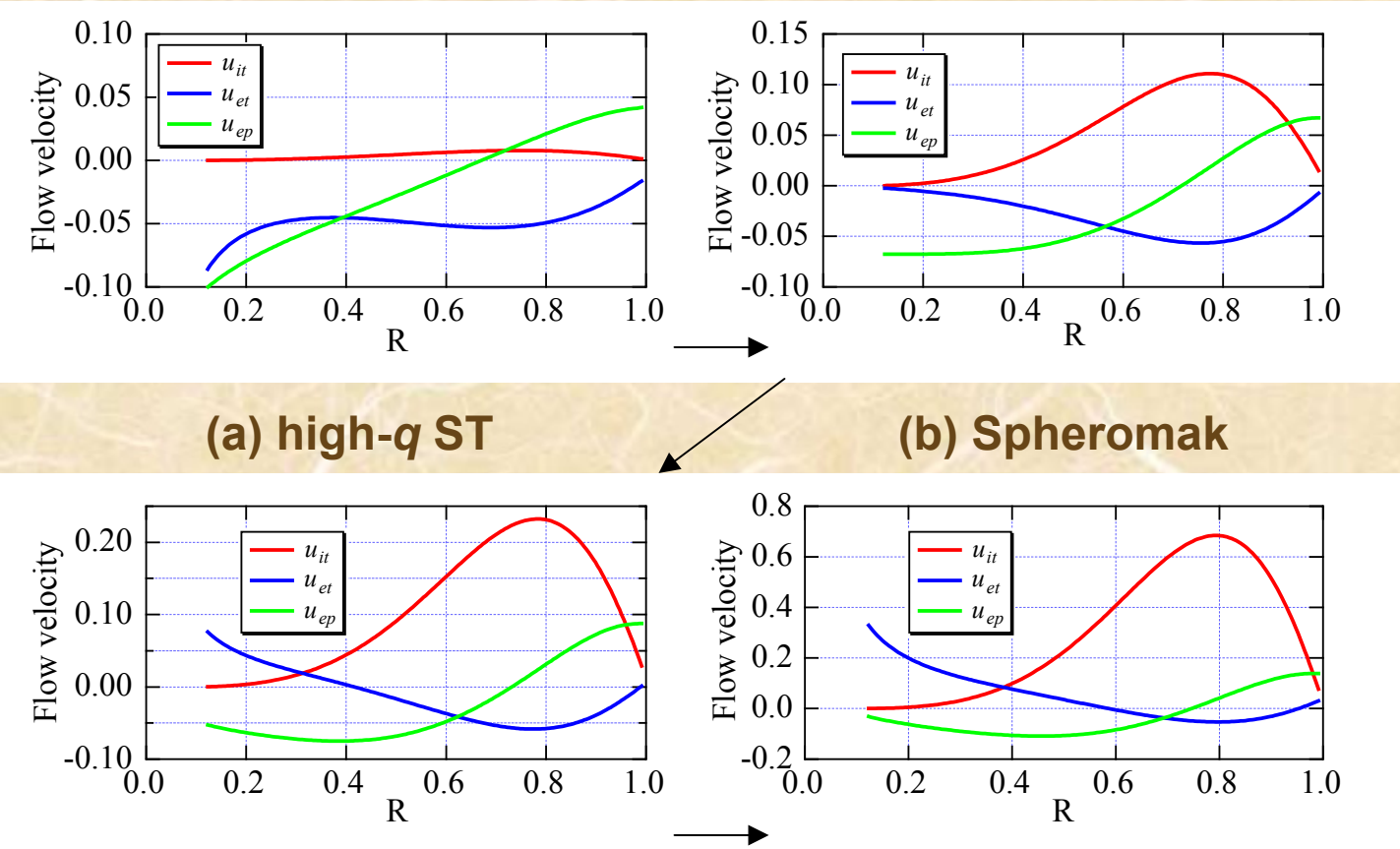

(a) high-*q* ST

(b) Spheromak

(c) RFP

(d) ultra low-*q* ST

--- You can see from Fig. (a) shows the toroidal current is dominantly carried by electron fluids. The electron fluids at the inner edge region are tied to $B_{t.e}$ while the ion fluids are not.

--- Figure (c) shows the electron flow at the inner edge region reverses the sign due to the reversal of $B_{t.e}$ at the inner edge region.

--- As the effect of the ion flow becomes more significant, the reversed region of the toroidal electron flow extends.

Toroidal current density and safety factor

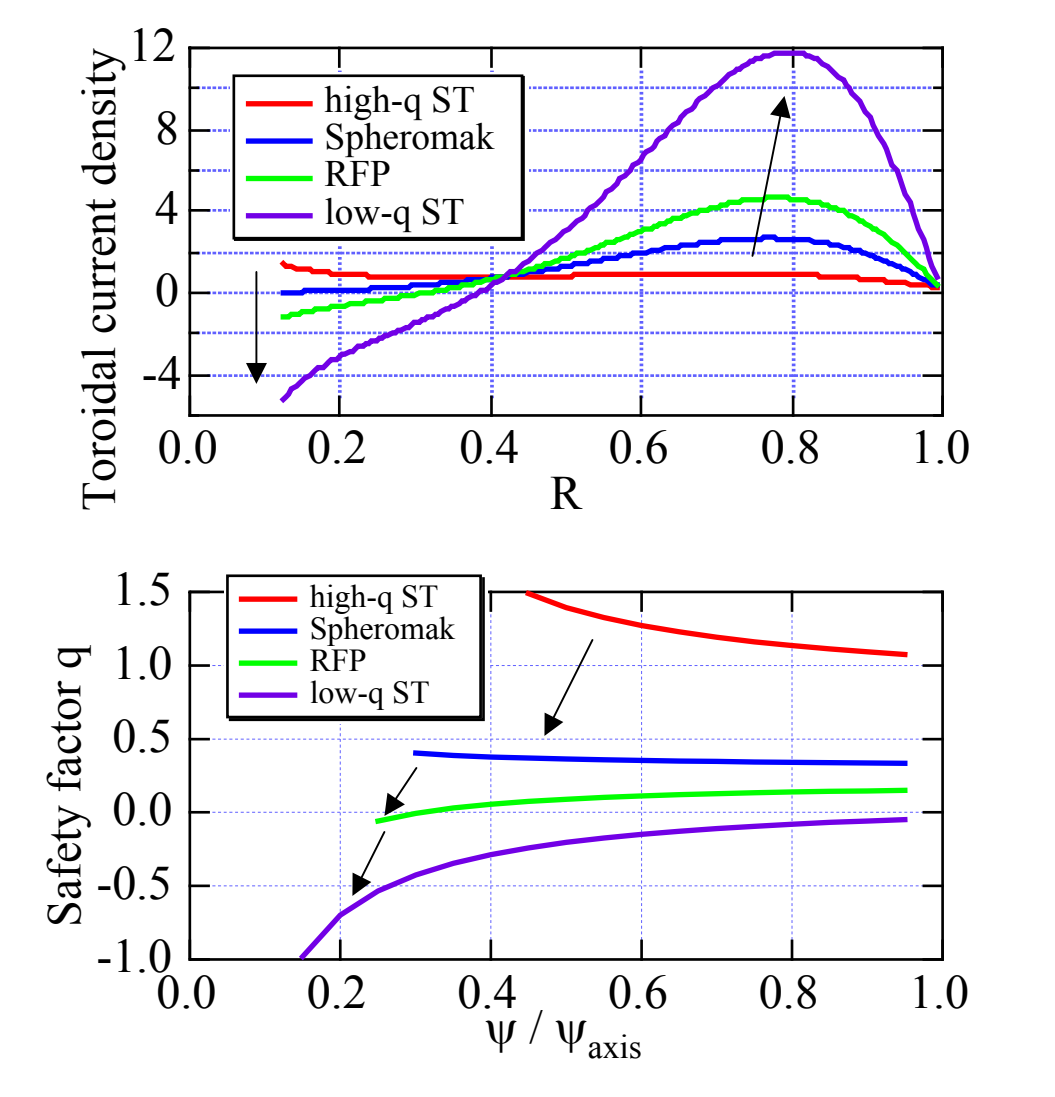

--- As the effect of ion flow becomes larger, the toroidal current density changes from the hollow profile to peaked one.
--- Further, due to the reversal of toroidal electron flow, it reverses the sign at the inner edge region.

--- We show the q-value as a function of the normalized poloidal flux function ψ / ψ_{axis}.
ψ_{axis} is ψ at the magnetic axis.
--- As the effect of ion flow becomes larger, the q-value comes down and reverses the sign at the inner edge region.
--- Finally, it reverses the sign at the whole region, and becomes the ultra low-*q*.

Poloidal flux contours

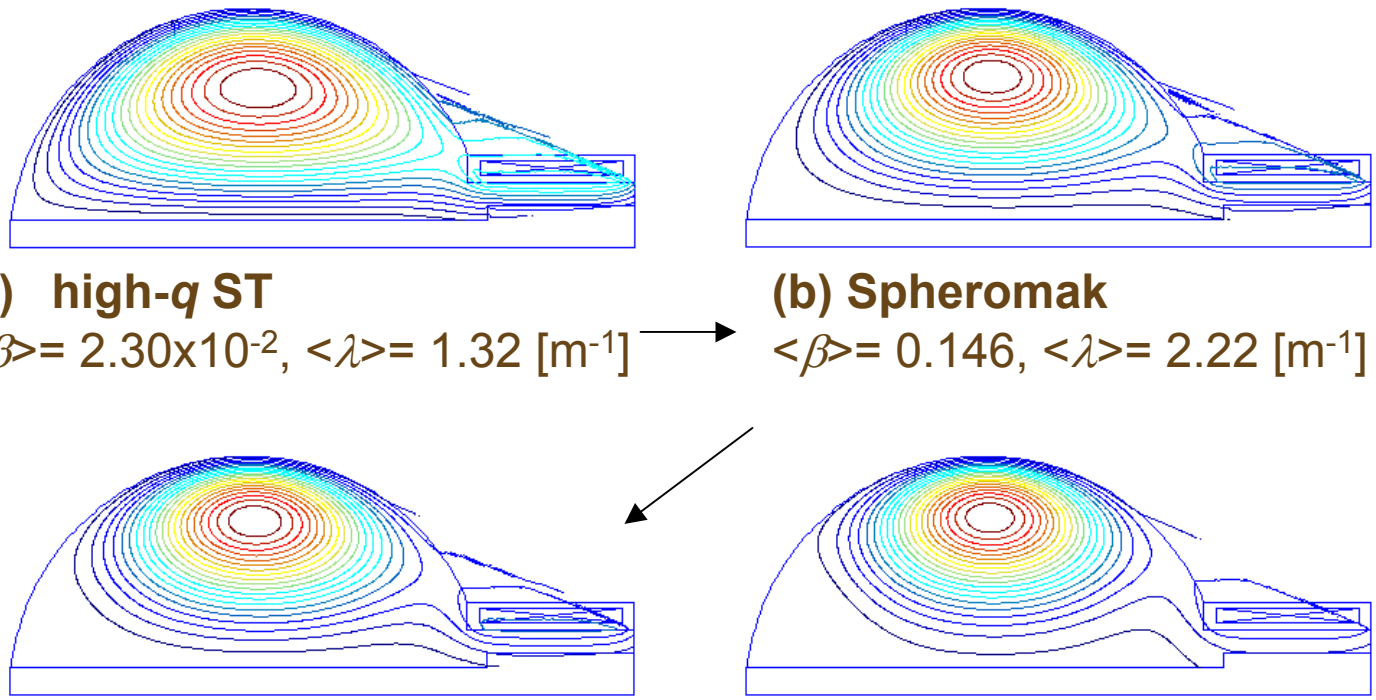

(a) high-*q* ST
$<\beta>$= 2.30x10^{-2}, $<\lambda>$= 1.32 [m^{-1}]

(b) Spheromak
$<\beta>$= 0.146, $<\lambda>$= 2.22 [m^{-1}]

(c) RFP
$<\beta>$= 0.230, $<\lambda>$= 2.24 [m^{-1}]

(d) ultra low-*q* ST
$<\beta>$= 0.179, $<\lambda>$= -0.673 [m^{-1}]

--- All these flux surfaces have the open flux penetrating the electrodes and form the helicity-driven configurations. This suggests the possibility of the current drive by CHI.

--- As the effect of ion flow becomes more significant, the amount of closed flux increases.

--- The STs have significantly lower $<\lambda>$ values than the spheromak and the RFP.

Note that the ultra low-*q* ST with diamagnetic B_t and high-β appears in the regime of $<\lambda>$ value lower than the lowest eigenvalue λ_e=9.29. Therefore, it could be observed in the experiment.

Beta <β> and two-fluid index f_{2F}

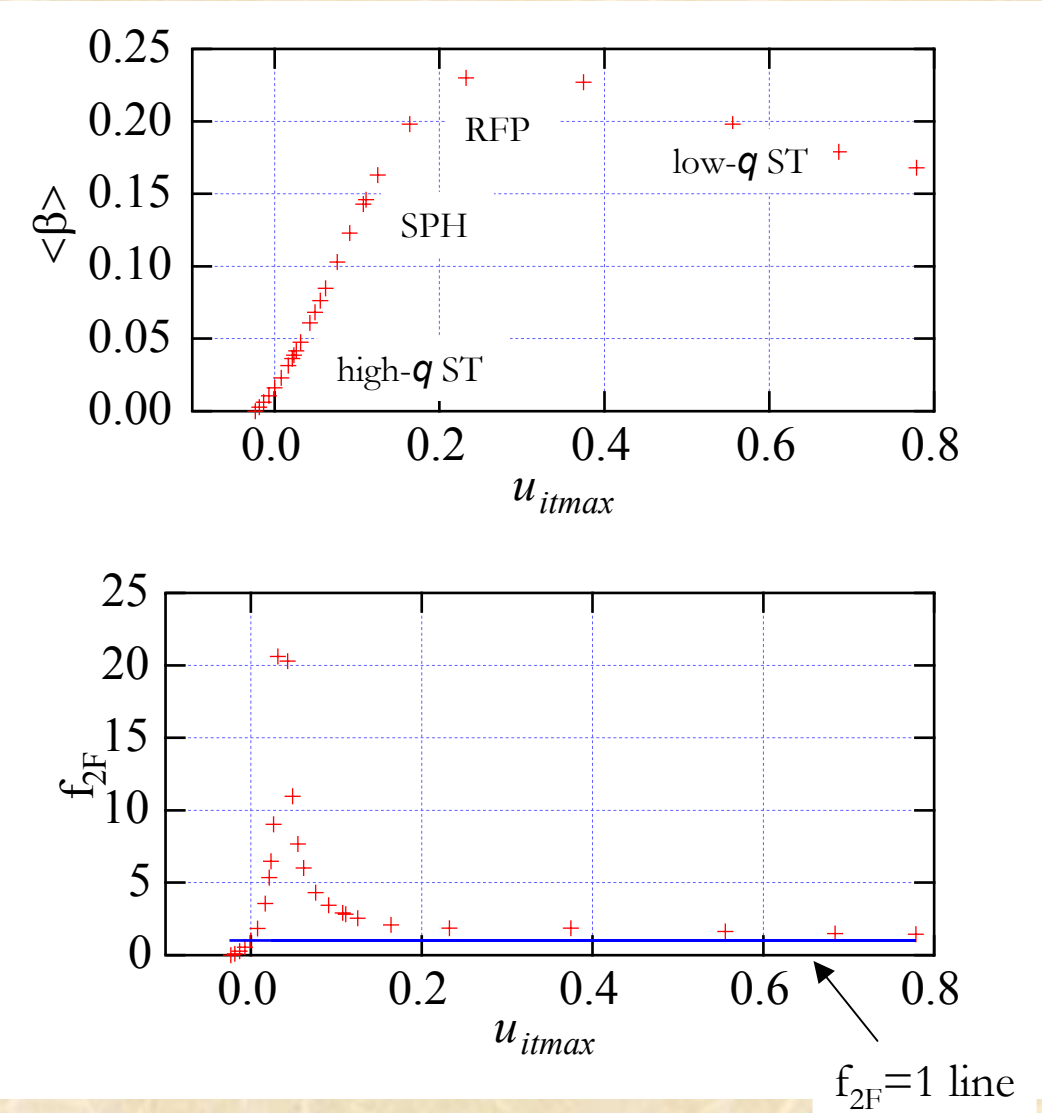

--- We examine the dependence of the maximum value of toroidal ion flow, u_{itmax} on the volume average beta value, <β>. As u_{itmax} increases by transition of high-q ST to RFP, <β> increases due to the decrease in $B_{t.e}$. On the other hand, <β> gradually decreases as u_{itmax} increases from the RFP to the ultra low-q ST.

--- Next, we examine u_{itmax} on the two-fluid index, f_{2F}. Except for the negative minimum values of u_{it}, all the values of f_{2F} are larger than unity. f_{2F} has a sharply peaked value in the slow ion flow region ($u_{it\,max} \approx 0.032$).

--- We consider why f_{2F} has the sharply peaked value.

Fluid drifts and profiles of $|F_{2F}|$, $S_*|u_i x B|$, and $|E|$

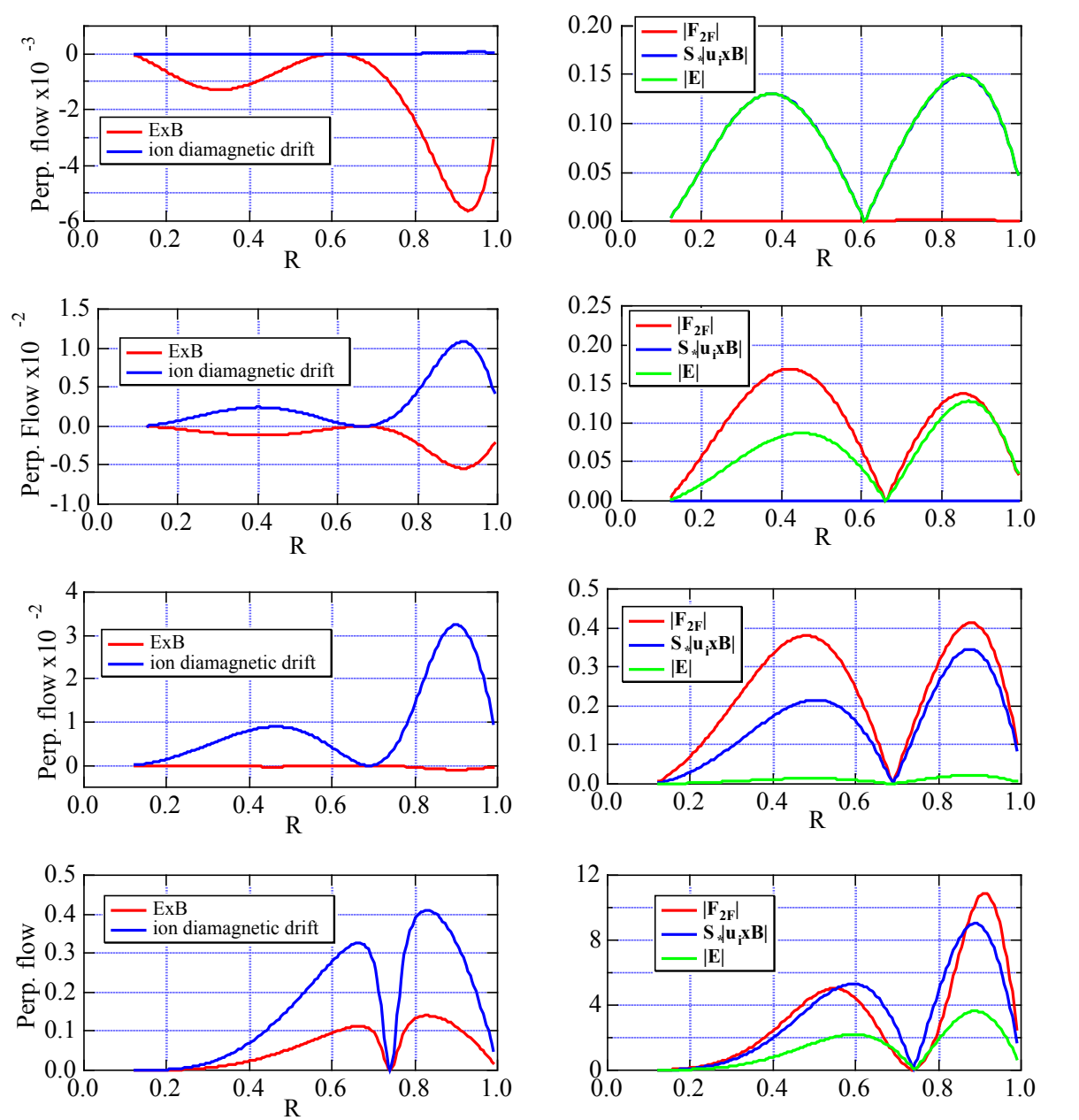

(a) u_{itmin}=-0.0234
ExB drift:dominant
Ion diamagnetic drift ~ zero

$$|\mathbf{E}| \approx S_* |\mathbf{u}_i \times \mathbf{B}| \longrightarrow \text{Single fluid}$$

(b) u_{itmax}=0

$$S_* |\mathbf{u}_i \times \mathbf{B}| = 0 \longrightarrow |\mathbf{E}| \approx S_* |\mathbf{F}_{2F}|$$

(c) u_{itmax}=0.032
ExB drift ~ zero
Ion diamagnetic drift :dominant

$$|\mathbf{E}| \approx 0 \longrightarrow S_* |\mathbf{u}_i \times \mathbf{B}| \approx |\mathbf{F}_{2F}|$$

$$f_{2F} \equiv \frac{<|\mathbf{F}_{2F} \times \mathbf{B}|>}{<|\mathbf{E} \times \mathbf{B}|>}$$:significantly large

(d) u_{itmax}=0.375

Summary

a) We have numerically determined the equilibrium of helicity-driven ST (HD-ST) based on the two-fluid model with flow.
b) The magnetic configurations change from the high-q ST (q>1) with paramagnetic toroidal field and low-β ($<\beta>\approx 2$ %) through the spheromak and the RFP to the ultra low-q ST ($0<q<1$) with diamagnetic toroidal field and high-β ($<\beta> \approx 18$ %) as the external toroidal field at the inner edge regions decreases and reverses the sign.
c) The ultra low-q ST appears in the regime of $<\lambda>$ value ($<\lambda>= -0.673$ m^{-1}) lower than the lowest eigenvalue λ_e=9.29. Therefore, it could be observed in the experiment.
d) The two-fluid effects are more significant in this equilibrium transition when the ion diamagnetic drift is dominant in the flowing two-fluid.

Future works

a) Confirmation of the conservation of the generalized helicities during this equilibrium transition.
b) Stability analysis of the flowing two-fluid equilibria of HD-ST.
c) How do we experimentally drive a flow of Alfven Mach number M_A~ 0.6 for producing the ultra low-q ST?

Fluid drifts perpendicular to magnetic field

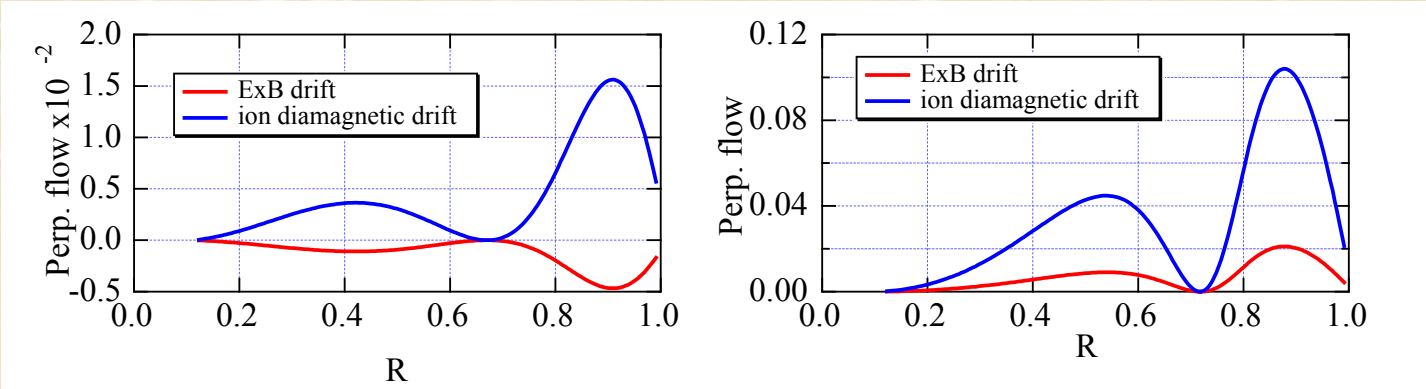

(a) high-*q* ST (b) Spheromak

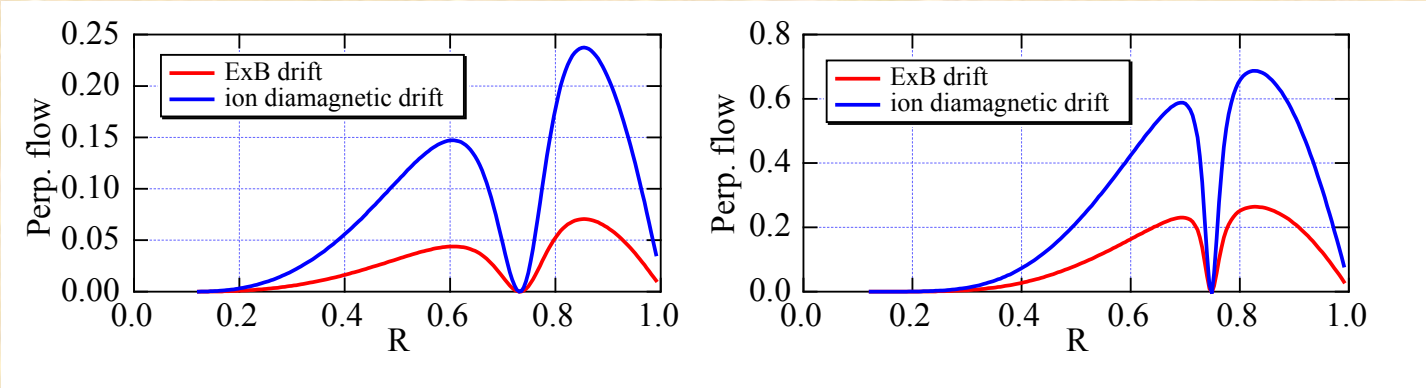

(c) RFP (d) ultra low-*q* ST

Profiles of $|F_{2F}|$, $S_*|u_i x B|$, and $|E|$

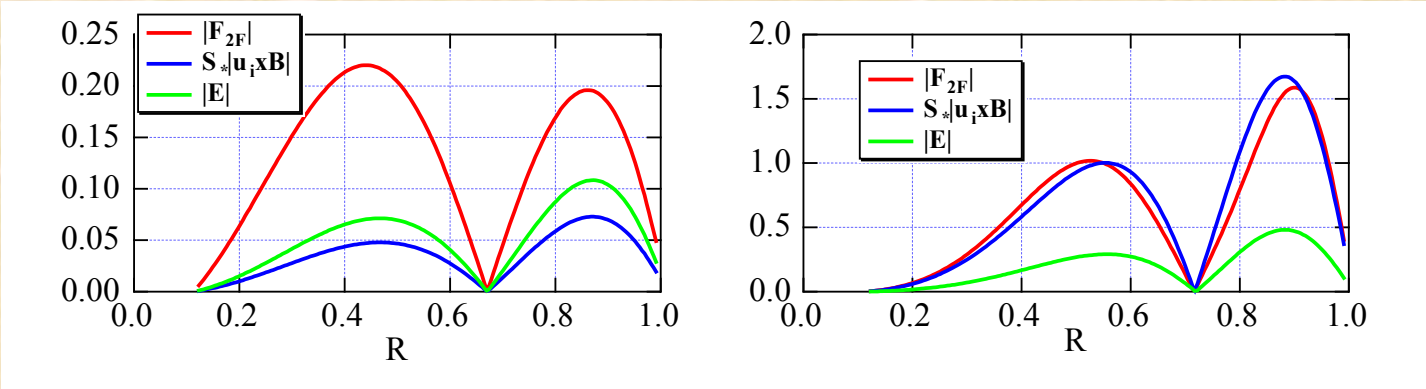

(a) high-*q* ST

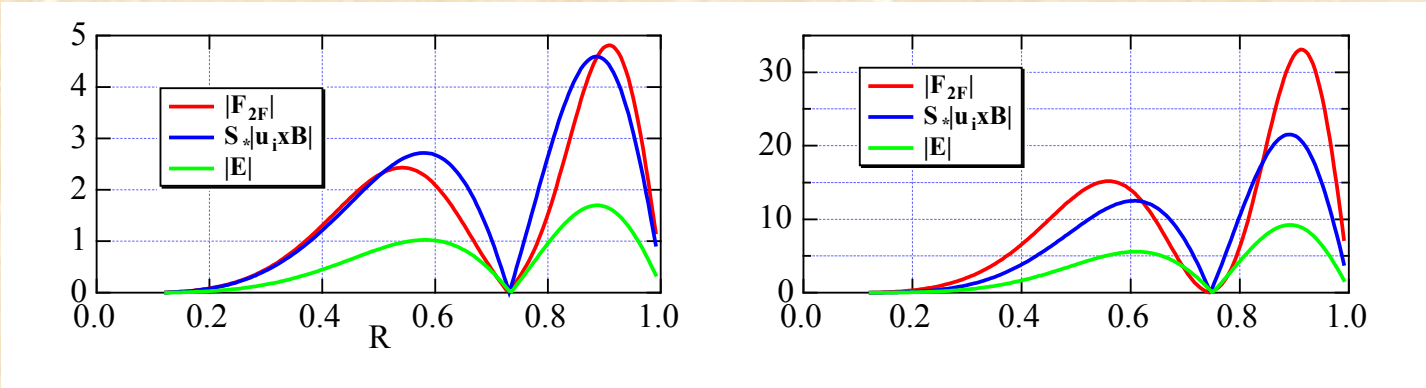

(b) Spheromak

(c) RFP

(d) ultra low-*q* ST